ACS APPLIED MATERIALS & INTERFACES

Research Article

www.acsami.org

Ultrasensitive and Selective Nitrogen Dioxide Sensor Based on Self-Assembled Graphene/Polymer Composite Nanofibers

Wenjing Yuan, Liang Huang, Qinqin Zhou, and Gaoquan Shi*

Department of Chemistry, Tsinghua University, Beijing 100084, People's Republic of China

Supporting Information

ABSTRACT: Reduced graphene oxide (rGO) sheets were self-assembled onto the surfaces of electrospun polymer nanofibers to form an ultrathin coating. These rGO/polymer composite nanofibers were used to fabricate nitrogen dioxide (NO_2) sensor. This sensor can be performed at room temperature, and it exhibited a high sensitivity of 1.03 ppm^{-1} with excellent selectivity and good reversibility. Furthermore, the limit of detection was experimentally measured to be as low as 150 ppb, and this value is much lower than the threshold exposure limit proposed by American Conference of Governmental Industrial Hygienists (200 ppb).

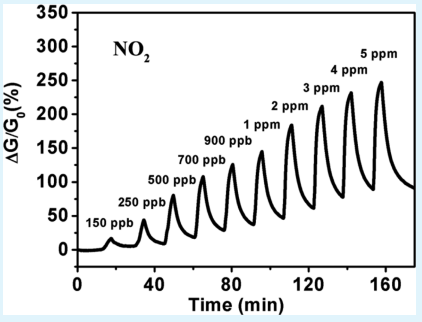

KEYWORDS: *reduced graphene oxide, gas sensor, nitrogen dioxide, self-assembly, electrospinning*

1. INTRODUCTION

Detection of hazardous gases is extremely important for personal safety protection and environmental monitoring.[1−5] NO_2 is a notorious gas mainly released by the emissions of fossil fuel combustion. It can cause acid rain that threatens the environment and respiratory problems in human beings.[6] National Institute for Occupational Safety and Health (NIOSH) published warnings about this toxic gas: NO_2 can induce immediately harm to life at concentrations higher than 20 ppm. Even under a low dose of exposure (1 ppm), NO_2 may cause headache, acute pulmonary edema, and irritations of eyes, nose, and throat. American Conference of Governmental Industrial Hygienists recommended a threshold exposure limit of 200 ppb NO_2 (https://www.osha.gov/dts/chemicalsampling/data/CH_257400.html). An ideal NO_2 sensor should have an experimental limit of detection (LOD) lower than this value. Besides, to develop a gas sensor for practical applications, its sensitivity, reversibility, selectivity, and energy consumption should also be considered and evaluated. Unfortunately, traditional chemiresistive gas sensors based on semiconducting oxides require to be operated at high temperatures in the range of 200−600 °C.[7] High temperatures need high power consumptions and possibly cause safety issues. Therefore, in recent years, extensive work has been devoted to the development of gas sensors that can be performed at room temperature. Graphene, a two-dimensional monolayer of carbon atoms packed into a honeycomb lattice,[8,9] is a unique and tempting sensing material for molecular detection.[10−12] This is mainly due to the fact that each of its atoms is a surface atom and the charge transport through a graphene sheet is highly sensitive to gas adsorption and desorption.[13,14] Actually, a variety of graphene materials have been explored for sensing NO_2, and the results are attractive.[15−19] Besides, graphene can provide a dimensionally compatible interface for the growth of cells to allow real-time detection of biointeresting molecules including nitric oxide released from living cells.[20,21] However, several serious problems still remain to be addressed before achieving a NO_2 sensor with practical importance. For example, graphene-based NO_2 sensors usually exhibit excellent sensitivities at high gas concentrations whereas they can seldom detect this gas with concentrations lower than 0.5 ppm without additional assistance.[22−25] The reversibility of most graphene-based sensors is also unsatisfactory. After exposure to NO_2, the sensing response can hardly return to its initial value in N_2 or air atmosphere without the treatment of heating or light irradiation.[26−29]

In this article, we report a facile and effective self-assembly technique for fabricating reduced graphene oxide/polymer composite nanofibers (rGO/P NFs). The NO_2 sensor based on these nanofibers showed a high sensitivity of 1.03 ppm^{-1} at room temperature with extremely low theoretical and experimental LODs of 17.5 and 150 ppb, respectively. Furthermore, it has a good selectivity, repeatability, and recoverability.

2. EXPERIMENTAL SECTION

2.1. Preparation of Polymer Nanofibers. A 9 wt % poly(vinyl alcohol) (PVA, M_W = 77 500, Sinopharm Chemical Reagent Co., Ltd.) solution was prepared by dissolving the polymer powder in deionized water at 98 °C under vigorous stirring. Then, this solution was mixed with an aqueous solution of poly(ether imide) (PEI, 30 wt %, M_W = 10 000, 99%, Alfa Aesar) to form a stable mixture with a PVA/PEI weight ratio of 4/1. Electrospinning of the mixed polymer solution was

Received: July 14, 2014
Accepted: September 10, 2014
Published: September 10, 2014

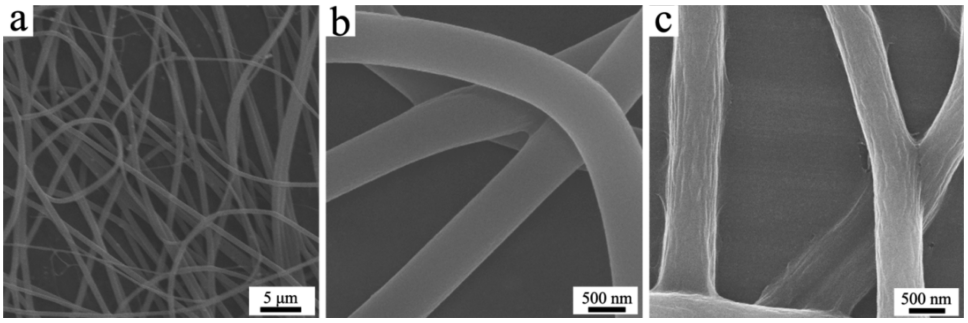

Figure 1. (a, b) SEM images of the electrospun GA cross-linked PVA/PEI nanofibers on Al foil before and (c) after assembling rGO sheets.

conducted at a 0.3 mL h^{-1} feeding rate using a syringe pump. The applied voltage was 20 kV. The fibers were deposited on substrate of a Al foil or an interdigitated electrode (IE, it has 6 parallel gold digits with a 25 μm spacing) at a 20 cm tip to collector distance. The freshly prepared fibers were then cross-linked by glutaraldehyde (GA) vapor overnight to improve their water stability.

2.2. Self-Assembly of GO Sheets. GO was synthesized using a modified Hummers' method from graphite powder, and the details are reported in the literature.[30,31] The as-obtained GO sheets in an aqueous dispersion were crushed for 15 min using an ultrasonic cell disruptor (JY88-II N Scientz, Ningbo Scientz Biotechnology Co., Ltd., Ningbo, China) and then diluted to 0.35 mg mL^{-1} for use. The positively charged PVA/PEI composite nanofibers along with their substrate were immersed into the GO solution for 10 min. After being washed with deionized water four times, the fibers were dried in air.

2.3. Chemical Reduction of Self-Assembled GO Sheets. The IE electrode bridged with the GO/P NFs was put into a vessel, and then an opened bottle containing 0.5 mL of hydrazine was placed neighboring the electrode. Successively, the vessel was sealed overnight for to reduce GO to conductive rGO by hydrazine vapor.

2.4. Sensing Test. All sensing tests were performed on a potentiostat−galvanostat (CHI 760D, CH Instruments Inc.). A two-electrode configuration was employed for all of the measurements. The sensitivity of the sensor was tested by applying a constant bias voltage of 1 V on the sensor and recording the conductance change. Before measurements, the gas chamber was purged with pure nitrogen gas (99.9%). After achieving a stable baseline, the sensor was exposed alternately to NO_2 and N_2. A mass flow controller was used to control the concentration of NO_2.

2.5. Characterizations. Raman spectra were recorded on a Renishaw Raman microscope (RM2000) with a 514 nm laser at a power density of 4.7 mW. X-ray photoelectron spectra (XPS) were taken out by using an ESCALAB 250 photoelectron spectrometer (ThermoFisher Scientific, U.S.). Scanning electron micrographs (SEM) were performed on a field-emission scanning electron microscope (Sirion-200, Japan). The atomic force microscopic (AFM) images of GO sheets were recorded by using a scanning probe microscope (SPM-9600, Shimadzu).

3. RESULTS AND DISCUSSION

3.1. Morphology and Structure of rGO/P NFs. Polymer nanofibers were prepared by electrospinning the mixed aqueous solution of PVA and PEI with a mass ratio of 4/1.[32] Then, the polymer chains of these nanofibers were chemically cross-linked with glutaraldehyde (GA) to improve their mechanical stability in aqueous media. Scanning electron microscope (SEM) images of the cross-linked PVA/PEI fibers indicate that they have smooth surfaces and an average diameter around 600 nm (Figure 1a and b). These fibers are positively charged in an aqueous medium because of their PEI component. Thus, the negatively charged GO sheets (ionization of residual carboxyl groups[33]) can be self-assembled onto the surfaces of polymer fibers upon electrostatic interaction. In order to make the sizes of GO sheets match the diameters of polymer fibers, the large GO sheets were cut by sonication to small pieces with lateral dimensions smaller than 2 μm, and most of them are around 1 μm (Supporting Information Figure S1a). The thicknesses of GO sheets were measured to be about 1.1 nm by AFM (Supporting Information Figure S2), and this value is in good agreement with those of GO monolayers.[34] This GO coating is nearly a monolayer because the excess physically adsorbed GO sheets were extensively removed by repeated washing with water. After self-assembly, the GO sheets were reduced with hydrazine vapor to restore their conductivity. X-ray photoelectron spectroscopic (XPS) measurements indicated that the C/O atomic ratio of GO was increased from 2.38 to 3.86 after the reduction because of partial removing of its oxygenated groups. As shown in Figure 1c, the outlines of cross-linked polymer nanofibers were well preserved after the treatments of self-assembly and chemical reduction of GO sheets. However, their surfaces exhibit wrinkles of rGO monolayer (Figure 1c, Supporting Information Figure S1b).

In the case of fabricating the NO_2 sensor, PVA/PEI nanofibers were electrospun on the surface of an IE (Supporting Information Figure S1c) and cross-linked with GA; successively, they were coated with rGO sheets through the same procedures described above. These rGO/P NFs bridged the gaps of the gold digits to form conductive channels (Figure 2a). The magnified scanning electron micrograph

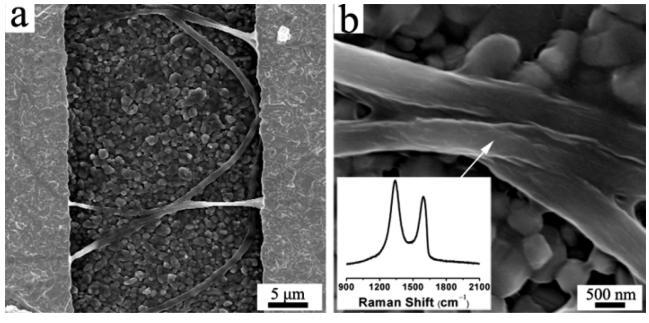

Figure 2. (a, b) SEM images of the surface of an rGO/P NFs bridged IE; inset of (b) is the Raman spectrum of the fiber surface.

(SEM) clearly shows the wrinkles of rGO coating on the surfaces of polymer nanofibers (Figure 2b). The Raman spectrum of rGO/P NFs also confirms the successful coating of rGO sheets (inset of Figure 2b). This spectrum displays a D-band at 1337 cm^{-1} and a G-band at 1593 cm^{-1}. The G-band is attributed to the first-order scattering of the E_{2g} mode. The D-band is associated with the structural defects related to the partially disordered structures of graphitic domains or created

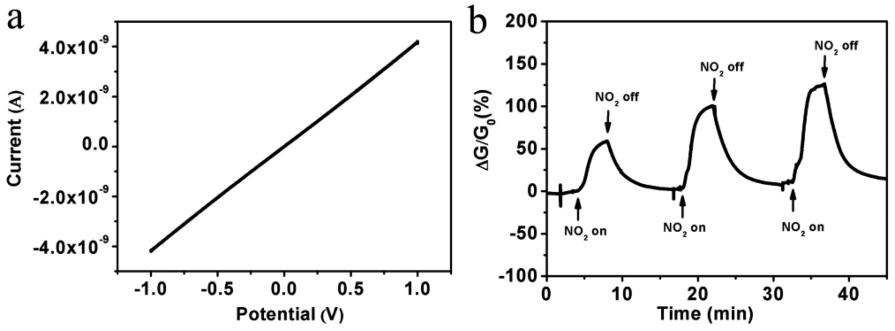

Figure 3. (a) Current versus voltage curve of the rGO/P NFs-based sensor. (b) Plot of response versus time for an rGO/P NFs-based sensor upon exposure to NO_2 gas with a concentration of 500 ppb, 1 ppm, or 2 ppm.

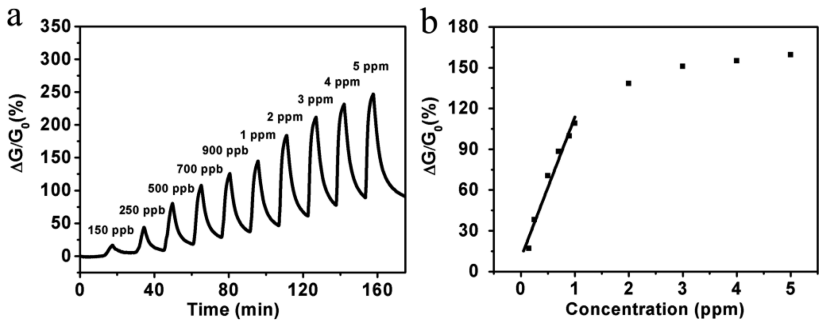

Figure 4. (a) Plot of response versus time for an rGO/P NFs-based sensor upon the exposure to NO_2 gas with concentrations ranging from 150 ppb to 5 ppm. (b) Response variation of rGO/P NFs-based sensor as a function of NO_2 concentration.

by the attachments of functional groups on the carbon basal plane.[16]

3.2. Performances of the NO_2 Sensor Based on rGO/P NFs. The current versus voltage (I–V) curve of an rGO/P NFs bridged IE exhibits an ohmic behavior (Figure 3a), and no hysteresis was observed throughout the test. The linear I–V relationship reflects that electrical contact plays a negligible role in the sensing process. The absence of Schottky barriers between rGO/P NFs and IE allows the accurate evaluation of the interactions between sensing layer and the target gas molecules.[35] This sensor exhibited excellent sensing performance at room temperature toward NO_2 gas. The sensing response (S) is defined as the ratio of conductance change of the sensor in target gas to that in pure N_2 ($S = G_{NO2}/G_{N2} - 1$). Before sensing, the device was set in a chamber deaerated by a N_2 flow until its response reached a flat baseline. The conductance of the sensor was found to increase upon the exposure to NO_2, which is consistent with the results reported previously.[28] rGO sheets have residual electron-withdrawing oxygenated groups; thus, they are a p-doped semiconductor. NO_2, an additional p-type dopant, can increase the hole-doping level and the conductance of rGO coating.[24] As shown in Figure 3b, the conductance of the sensor undergoes a drastic increase after exposing to the target gas, and it can also decline nearly to its initial value after blowing N_2 for several minutes. The time required to reach 90% of the maximum response upon exposing to 500 ppb NO_2 (t_{90}) was shorter than 3 min, and the time needed for decreasing the saturated response to 10% by blowing pure N_2 (t_{10}) was less than 6 min. Therefore, we used an exposure time of 4 min and a recovery time of 10 min for carrying out all our gas sensing experiments to have a fair comparison. Moreover, these time periods are reasonable for a practical sensor.

The responses of this sensor upon exposing to NO_2 gases with concentrations ranging from 150 ppb to 5 ppm are recorded in Figure 4a. Only a small drift of baseline was observed during the multiple cycling process. After exposure to 150 ppb NO_2 for 4 min, the conductance of this sensor was increased by 16.5%. The sensing response increased with the increase of NO_2 concentration. For example, a high conductance increase of 159.4% was observed at 5 ppm of NO_2. The sensing response is linearly proportional to NO_2 concentration in the region of lower than 1 ppm (Figure 4b). Higher NO_2 concentration caused partial saturation, and the conductance response distorted from linearity. The sensitivity of this sensor was calculated to be as high as 1.03 ppm^{-1} (response slope of the fitting line). The theoretical LOD of this sensor was calculated to be approximately 17.5 ppb based on its signal (S) to noise (N) ratio (S/N = 3). It should be noted here that the experimental LOD of this sensor was measured to be 150 ppb. This value is well below the threshold exposure limit proposed by American Conference of Governmental Industrial Hygienists (200 ppb) as described above, implying that our sensor is suitable for practical application. For comparison, we intentionally coated a thicker rGO film on the polymer fibers by keeping the excess physically adsorbed GO sheets (without washing) in the self-assembly step. However, the sensor prepared by reducing the unwashed GO/P NFs showed a response to NO_2 gas 2.4 times weaker than that of the washed counterpart (Supporting Information Figure S3). The sensor with a drop-casted rGO film (1.5 μL 0.03 mg mL^{-1} GO solution casted on a 0.04 cm^2 IE and reduced with hydrazine vapor) exhibited only 13% conductance change upon exposure to 500 ppb NO_2. Furthermore, the PVA/PEI nanofibers are electrically insulating; thus, they cannot be applied for the fabrication of chemiresistive gas sensor without rGO coatings. The superior performance of this gas sensor is ascribed to the

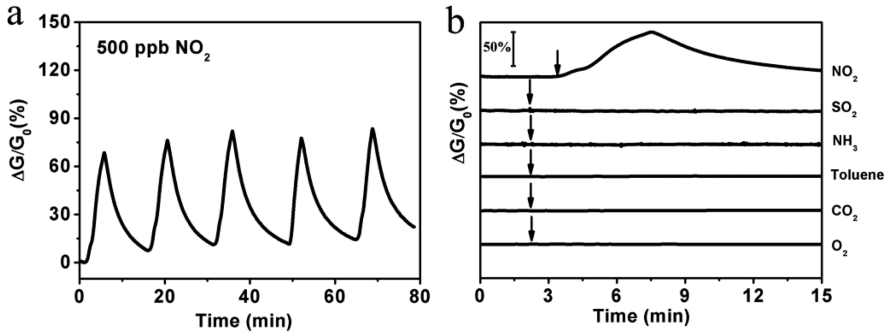

Figure 5. (a) Conductance changes of an rGO/P NFs-based sensor during 5 successive cycles of alternative exposure to 500 ppb NO_2 for 4 min and N_2 flow for 10 min. (b) Response of an rGO/P NFs-based sensor to 500 ppb NO_2, 5 ppm of SO_2, 300 ppm of NH_3, 10% toluene, 10% CO_2, or 10% O_2; arrows indicate the time of inducing the target gases.

Table 1. Performance Comparison of the NO_2 Sensors Based on Different Graphene Materials

graphene material	sensitivity (1/ppm)	exptl LOD (ppm)	response time (min)	recover time (min)	ref
rGO/P NFs	1.03	0.15	4	10	this work
graphene	0.02 at 5 ppm	5.00	5	10−12 in humid air	41
chemically modified rGO	0.44	2.00	10	30	35
graphene nanomesh	0.04	1.00	15	20 unrecoverable	43
rGO bonded to Au electrode	0.01	1.00	7	28	42
rGO	0.09 at 100 ppm	–	15	25 unrecoverable	32
rGO/SnO_2	0.03 at 100 ppm	1.00	1.1	unrecoverable	44
rGO/Au nanoparticles	0.07	0.20	5−6	11 unrecoverable	45
rGO/polymer 3D scaffold	0.28 at 0.25 ppm	–	7−8	13 unrecoverable	46

synergetic effect of the ultrathin rGO layer formed by self-assembly and its underneath polymer nanofibers. The active surface areas of sensing materials have strong effects on their performances including sensitivities, LODs, and recoverability.[6] The widely used traditional techniques such as drop casting,[36] spin coating,[28] and inkjet printing[17] can only fabricate relatively thick rGO membranes, consisting of several tens or even hundreds of layers of rGO sheets. However, the self-assembly method described here produced a nearly monolayer rGO membrane, and the excess physically adsorbed rGO sheets were removed by washing. Therefore, all the rGO sheets were exposed to the target gas; the adsorption of a small amount of NO_2 strongly increased the conductance of rGO membrane. Furthermore, as NO_2 molecules adsorbed at the edges of rGO sheets, the junction resistances between rGO sheets would change greatly, enhancing the sensitivity of this sensor. On the other hand, the polymer nanofibers are an additional absorbent of NO_2, concentrating the gas molecules on the surface of rGO monolayer. Furthermore, polymer nanofibers can also increase the doping level and enhance the carrier scattering of graphene to improve the performance of our gas sensor.[37]

The rGO/P NFs-based sensor was exposed to 500 ppb NO_2 for five successive cycles (exposing time = 4 min for each cycle), and stable sensing signals with a response of approximately 68% were recorded (Figure 5a). When the NO_2 flow was turned off and a N_2 flow was introduced, the conductance of the sensor recovered close to its initial value within 10 min. These results suggest that this sensor has a good repeatability. Many of the graphene or rGO-based NO_2 sensors need the aid of photoillumination or thermal treatment to recover their initial states.[28,29] In contrast, our sensor exhibited good signal repeatability simply by blowing N_2 gas at room temperature.

Selectivity is another key parameter for gas sensors. Figure 5b shows the responses of the rGO/P NFs-based sensor toward different target gases. Reducing gas sulfur dioxide (SO_2) and ammonia (NH_3), aromatic organic vapor of toluene, and common interfering gases including oxygen (O_2) and carbon dioxide (CO_2) have been studied. This sensor exhibited high response to NO_2 gas and nearly no responses to those possible interferential gases. These phenomena can be explained as follows. Conductance change of the sensor is caused by the charge transfer between graphene sheets and target molecules. Theoretical calculations revealed that the charge transfer between NO_2 molecules and graphene is much more energy favorable than those between NH_3, CO_2, or O_2 molecules and graphene.[38,39] Particularly, defective graphene (e.g., rGO) can strongly and selectively interact with NO_2.[40] Toluene molecules can adsorb on graphene through $\pi-\pi$ interaction, but the resultant charge transfer is extremely weak. The strong interaction between electron-donating groups of PEI (−NH−) and electron-withdrawing NO_2 molecules can also enhance the response of rGO/P NFs-based sensor. Negligible cross-sensitivities of possible interfering gases make our gas sensor promising for practical applications under ambient conditions.

The performance of the rGO/P NFs-based NO_2 sensor is compared with those of other graphene-based counterparts reported in the literature (Table 1). All sensing devices listed in Table 1 were tested at room temperature. The sensitivity of our rGO/P NFs-based sensor is 2−30 times higher than those of the sensors based on graphene or rGO,[36,41] chemically modified rGO,[35] rGO covalently bonded to Au electrode,[42] graphene nanomesh,[43] and rGO/metal,[44] rGO/metal oxide,[45] or rGO/3D polymer scaffold composites.[46] The experimental LOD reported here is 150 ppb, and this value is much lower than those of the other sensors described above. Last but not

least, our sensor is able to be recovered to its initial state within 10 min just by blowing N_2, and this time is much shorter than those of the other sensors performing in the same environment. Furthermore, several graphene-based NO_2 sensors are unrecoverable. The high-performance of the NO_2 sensor based on rGO/P NFs is attributed to the easy accessibility of rGO surface to gas molecules. The self-assembled rGO membrane is nearly a monolayer, much thinner than those of the counterparts prepared by drop-casting or inkjet printing. A thick sensing membrane restricts the desorption of the gas molecules adsorbed in its bulk matrix, elongating the recovery time of sensors. The rGO/P NFs-based NO_2 sensors were fabricated by the combination of electrospinning and self-assembly; thus, the method developed here is simpler and cheaper compared with the techniques based on microfabrication or thermal evaporation.

4. CONCLUSIONS

rGO/P NFs have been successfully prepared by self-assembling GO sheets onto the surfaces of electrospun PVA/PEI NFs in an aqueous medium followed by chemical reduction. This technique is simple, cheap, and eco-friendly. The NO_2 sensor based on these rGO/P NFs showed a high sensitivity, an extremely low LOD, fast response and recovery, good repeatability, and excellent selectivity. This high-performance gas sensor can be performed at room temperature without any other assistance, promising for practical applications.

■ ASSOCIATED CONTENT

Supporting Information

SEM images of the GO sheets and IE. This material is available free of charge via the Internet at http://pubs.acs.org.

■ AUTHOR INFORMATION

Corresponding Author

*Tel.: (+86) 10 62773743. Fax: (+86) 10 62771149. E-mail: gshi@tsinghua.edu.cn.

Author Contributions

The manuscript was written through contributions of all authors. All authors have given approval to the final version of the manuscript.

Notes

The authors declare no competing financial interest.

■ ACKNOWLEDGMENTS

This work was supported by National Basic Research Program of China (973 Program, 2012CB933402, 2013CB933001) and Natural Science Foundation of China (51433005, 51161120361,).

■ REFERENCES

(1) He, Q. Y.; Wu, S. X.; Yin, Z. Y.; Zhang, H. Graphene-Based Electronic Sensors. *Chem. Sci.* **2012**, *3*, 1764−1772.

(2) Liu, Y. X.; Dong, X. C.; Chen, P. Biological and Chemical Sensors Based on Graphene Materials. *Chem. Soc. Rev.* **2012**, *41*, 2283−2307.

(3) Basu, S.; Bhattacharyya, P. Recent Developments on Graphene and Graphene Oxide Based Solid State Gas Sensors. *Sens. Actuators, B* **2012**, *173*, 1−21.

(4) Ratinac, K. R.; Yang, W.; Ringer, S. P.; Braet, F. Toward Ubiquitous Environmental Gas Sensors—Capitalizing on the Promise of Graphene. *Environ. Sci. Technol.* **2010**, *44*, 1167−1176.

(5) Li, W. W.; Geng, X. M.; Guo, Y. F.; Rong, J. Z.; Gong, Y. P.; Wu, L. Q.; Zhang, X. M.; Li, P.; Xu, J. B.; Cheng, G. S.; Sun, M. T.; Liu, L. W. Reduced Graphene Oxide Electrically Contacted Graphene Sensor for Highly Sensitive Nitric Oxide Detection. *ACS Nano* **2011**, *5*, 6955−6961.

(6) Liu, H.; Li, M.; Voznyy, O.; Hu, L.; Fu, Q.; Zhou, D.; Xia, Z.; Sargent, E. H.; Tang, J. Physically Flexible, Rapid-Response Gas Sensor Based on Colloidal Quantum Dot Solids. *Adv. Mater.* **2014**, *26*, 2718−2724.

(7) Choi, S. J.; Jang, B. H.; Lee, S. J.; Min, B. K.; Rothschild, A.; Kim, I. D. Selective Detection of Acetone and Hydrogen Sulfide for the Diagnosis of Diabetes and Halitosis Using SnO_2 Nanofibers Functionalized with Reduced Graphene Oxide Nanosheets. *ACS Appl. Mater. Interfaces* **2014**, *6*, 2587−2596.

(8) Huang, C. C.; Li, C.; Shi, G. Q. Graphene Based Catalysts. *Energy Environ. Sci.* **2012**, *5*, 8848−8868.

(9) Cong, H.-P.; Ren, X.-C.; Wang, P.; Yu, S.-H. Macroscopic Multifunctional Graphene-Based Hydrogels and Aerogels by a Metal Ion Induced Self-Assembly Process. *ACS Nano* **2012**, *6*, 2693−2703.

(10) Huang, L.; Wang, Z. P.; Zhang, J. K.; Pu, J. L.; Lin, Y. J.; Xu, S. H.; Shen, L.; Chen, Q.; Shi, W. Z. Fully Printed, Rapid-Response Sensors Based on Chemically Modified Graphene for Detecting NO_2 at Room Temperature. *ACS Appl. Mater. Interfaces* **2014**, *6*, 7426−7433.

(11) Li, W.; Geng, X.; Guo, Y.; Rong, J.; Gong, Y.; Wu, L.; Zhang, X.; Li, P.; Xu, J.; Cheng, G.; Sun, M.; Liu, L. Reduced Graphene Oxide Electrically Contacted Graphene Sensor for Highly Sensitive Nitric Oxide Detection. *ACS Nano* **2011**, *5*, 6955−6961.

(12) Robinson, J. T.; Perkins, F. K.; Snow, E. S.; Wei, Z.; Sheehan, P. E. Reduced Graphene Oxide Molecular Sensors. *Nano Lett.* **2008**, *8*, 3137−3140.

(13) Schedin, F.; Geim, A. K.; Morozov, S. V.; Hill, E. W.; Blake, P.; Katsnelson, M. I.; Novoselov, K. S. Detection of Individual Gas Molecules Adsorbed on Graphene. *Nat. Mater.* **2007**, *6*, 652−655.

(14) Crowther, A. C.; Ghassaei, A.; Jung, N.; Brus, L. E. Strong Charge-Transfer Doping of 1 to 10 Layer Graphene by NO_2. *ACS Nano* **2012**, *6*, 1865−1875.

(15) Yavari, F.; Koratkar, N. Graphene-Based Chemical Sensors. *J. Phys. Chem. Lett.* **2012**, *3*, 1746−1753.

(16) Yuan, W. J.; Shi, G. Q. Graphene-Based Gas Sensors. *J. Mater. Chem. A* **2013**, *1*, 10078−10091.

(17) Dua, V.; Surwade, S. P.; Ammu, S.; Agnihotra, S. R.; Jain, S.; Roberts, K. E.; Park, S.; Ruoff, R. S.; Manohar, S. K. All-Organic Vapor Sensor Using Inkjet-Printed Reduced Graphene Oxide. *Angew. Chem., Int. Ed.* **2010**, *49*, 2154−2157.

(18) Deng, S.; Tjoa, V.; Fan, H. M.; Tan, H. R.; Sayle, D. C.; Olivo, M.; Mhaisalkar, S.; Wei, J.; Sow, C. H. Reduced Graphene Oxide Conjugated Cu_2O Nanowire Mesocrystals for High-Performance NO_2 Gas Sensor. *J. Am. Chem. Soc.* **2012**, *134*, 4905−4917.

(19) Han, T. H.; Huang, Y. K.; Tan, A. T. L.; Dravid, V. P.; Huang, J. X. Steam Etched Porous Graphene Oxide Network for Chemical Sensing. *J. Am. Chem. Soc.* **2011**, *133*, 15264−15267.

(20) Guo, C. X.; Zheng, X. T.; Lu, Z. S.; Lou, X. W.; Li, C. M. Biointerface by Cell Growth on Layered Graphene−Artificial Peroxidase−Protein Nanostructure for in Situ Quantitative Molecular Detection. *Adv. Mater.* **2010**, *22*, 5164−5167.

(21) Guo, C. X.; Ng, S. R.; Khoo, S. Y.; Zheng, X.; Chen, P.; Li, C. M. RGD-Peptide Functionalized Graphene Biomimetic Live-Cell Sensor for Real-Time Detection of Nitric Oxide Molecules. *ACS Nano* **2012**, *6*, 6944−6951.

(22) Kang, I.-S.; So, H.-M.; Bang, G.-S.; Kwak, J.-H.; Lee, J.-O.; Ahn, C. W. Recovery Improvement of Graphene-Based Gas sensors Functionalized with Nanoscale Heterojunctions. *Appl. Phys. Lett.* **2012**, *101*, 123504−123507.

(23) Lu, G. H.; Ocola, L. E.; Chen, J. H. Gas Detection Using Low-Temperature Reduced Graphene Oxide Sheets. *Appl. Phys. Lett.* **2009**, *94*, 083111−083113.

(24) Nomani, M. W. K.; Shishir, R.; Qazi, M.; Diwan, D.; Shields, V. B.; Spencer, M. G.; Tompa, G. S.; Sbrockey, N. M.; Koley, G. Highly Sensitive and Selective Detection of NO_2 Using Epitaxial Graphene on 6H-SiC. *Sens. Actuators, B* **2010**, *150*, 301−307.

(25) Yu, K. H.; Wang, P. X.; Lu, G. H.; Chen, K. H.; Bo, Z.; Chen, J. H. Patterning Vertically Oriented Graphene Sheets for Nanodevice Applications. *J. Phys. Chem. Lett.* **2011**, *2*, 537−542.
(26) Joshi, R. K.; Gomez, H.; Alvi, F.; Kumar, A. Graphene Films and Ribbons for Sensing of O_2, and 100 ppm of CO and NO_2 in Practical Conditions. *J. Phys. Chem. C* **2010**, *114*, 6610−6613.
(27) Strong, V.; Dubin, S.; El-Kady, M. F.; Lech, A.; Wang, Y.; Weiller, B. H.; Kaner, R. B. Patterning and Electronic Tuning of Laser Scribed Graphene for Flexible All-Carbon Devices. *ACS Nano* **2012**, *6*, 1395−1403.
(28) Fowler, J. D.; Allen, M. J.; Tung, V. C.; Yang, Y.; Kaner, R. B.; Weiller, B. H. Practical Chemical Sensors from Chemically Derived Graphene. *ACS Nano* **2009**, *3*, 301−306.
(29) Chen, G. G.; Paronyan, T. M.; Harutyunyan, A. R. Sub-ppt Gas Detection with Pristine Graphene. *Appl. Phys. Lett.* **2012**, *101*, 053119−053123.
(30) Xu, Y. X.; Zhao, L.; Bai, H.; Hong, W. J.; Li, C.; Shi, G. Q. Chemically Converted Graphene Induced Molecular Flattening of 5,10,15,20-Tetrakis(1-methyl-4-pyridinio) Porphyrin and Its Application for Optical Detection of Cadmium(II) Ions. *J. Am. Chem. Soc.* **2009**, *131*, 13490−13497.
(31) Hummers, W. S.; Offeman, R. E. Preparation of Graphitic Oxide. *J. Am. Chem. Soc.* **1958**, *80*, 1339−1339.
(32) Wang, X.; Ding, B.; Sun, M.; Yu, J.; Sun, G. Nanofibrous Polyethyleneimine Membranes as Sensitive Coatings for Quartz Crystal Microbalance-Based Formaldehyde Sensors. *Sens. Actuators, B* **2010**, *144*, 11−17.
(33) Huang, X.; Qi, X.; Boey, F.; Zhang, H. Graphene-Based Composites. *Chem. Soc. Rev.* **2012**, *41*, 666−686.
(34) Xu, Y. X.; Bai, H.; Lu, G. W.; Li, C.; Shi, G. Q. Flexible Graphene Films via the Filtration of Water-Soluble Noncovalent Functionalized Graphene Sheets. *J. Am. Chem. Soc.* **2008**, *130*, 5856−5857.
(35) Yuan, W. J.; Liu, A. R.; Huang, L.; Li, C.; Shi, G. Q. High-Performance NO_2 Sensors Based on Chemically Modified Graphene. *Adv. Mater.* **2012**, *5*, 766−771.
(36) Lu, G. H.; Park, S. G.; Yu, K. H.; Ruoff, R. S.; Ocola, L. E.; Rosenmann, D.; Chen, J. H. Toward Practical Gas Sensing with Highly Reduced Graphene Oxide: A New Signal Processing Method to Circumvent Run-to-Run and Device-to-Device Variations. *ACS Nano* **2011**, *5*, 1154−1164.
(37) Dan, Y. P.; Lu, Y.; Kybert, N. J.; Luo, Z. T.; Johnson, A. T. C. Intrinsic Response of Graphene Vapor Sensors. *Nano Lett.* **2009**, *9*, 1472−1475.
(38) Duan, W.; Gu, B.-L.; Wu, J.; Hao, S.; Zhou, G.; Liu, Z.; Li, Z.; Huang, B. Adsorption of Gas Molecules on Graphene Nanoribbons and Its Implication for Nanoscale Molecule Sensor. *J. Phys. Chem. C* **2008**, *112*, 13442−13446.
(39) Leenaerts, O.; Partoens, B.; Peeters, F. M. Adsorption of H_2O, NH_3, CO, NO_2, and NO on Graphene: A First-Principles Study. *Phys. Rev. B* **2008**, *77*, 125416−125421.
(40) Zhang, Y.-H.; Chen, Y.-B.; Zhou, K.-G.; Liu, C.-H.; Zeng, J.; Zhang, H.-L.; Peng, Y. Improving Gas Sensing Properties of Graphene by Introducing Dopants and Defects: A First-Principles Study. *Nanotechnology* **2009**, *20*, 185504.
(41) Randeniya, L. K.; Shi, H. Q.; Barnard, A. S.; Fang, J. H.; Martin, P. J.; Ostrikov, K. Harnessing the Influence of Reactive Edges and Defects of Graphene Substrates for Achieving Complete Cycle of Room-Temperature Molecular Sensing. *Small* **2013**, *9*, 3993−3999.
(42) Su, P. G.; Shieh, H. C. Flexible NO_2 Sensors Fabricated by Layer-by-Layer Covalent Anchoring and in Situ Reduction of Graphene Oxide. *Sens. Actuators, B* **2014**, *190*, 865−872.
(43) Paul, R. K.; Badhulika, S.; Saucedo, N. M.; Mulchandani, A. Graphene Nanomesh as Highly Sensitive Chemiresistor Gas Sensor. *Anal. Chem.* **2012**, *84*, 8171−8178.
(44) Mao, S.; Cui, S.; Lu, G. h.; Yu, K. h.; Wen, Z. h.; Chen, J. H. Tuning Gas-Sensing Properties of Reduced Graphene Oxide Using Tin Oxide Nanocrystals. *J. Mater. Chem.* **2012**, *22*, 11009−11013.
(45) Verawati, T.; Wei, J.; Vinayak, D.; Subodh, M.; Nripan, M. Hybrid Graphene−Metal Nanoparticle Systems: Electronic Properties and Gas Interaction. *J. Mater. Chem.* **2011**, *21*, 15593−15599.
(46) Yun, Y. J.; Hong, W. G.; Choi, N.-J.; Park, H. J.; Moon, S. E.; Kim, B. H.; Song, K.-B.; Jun, Y.; Lee, H.-K. A 3D Scaffold for Ultra-Sensitive Reduced Graphene Oxide Gas Sensors. *Nanoscale* **2014**, *6*, 6511−6514.